Z-99 Visualized connections between seismic inversion and prestack seismic migration

JOHN C. BANCROFT
Department of Geology and Geophysics,
University of Calgary,
Calgary, Alberta,
Canada, T2N 1N4

SUMMARY

The Kirchhoff migration algorithm is heuristically derived using the mathematics of least squares inversion and the concept of matched filters. These concepts are visualized with cartoon descriptions that describe inversion using linear algebra and commences with time-varying deconvolution. The time varying wavelets are then replaced with diffractions, to form a diffraction matrix that is used to model variable offset seismic data. The product of the transpose of this diffraction matrix with the seismic data produces a band-limited inversion that is identical to a Kirchhoff migration. Simple modification to the diffraction matrix illustrate the use of variable velocities and constant offset prestack migration.

INTRODUCTION

The term inversion is used with a number of different processes and applications in geophysics such as:

1. Estimating the source and receiver statics from cross-correlation statics (residuals and trims)
2. Deconvolution of seismic traces
3. Converting seismic data to a geological image or estimating rock properties.

These applications often use the mathematics of least squares inversion, where observations are processed to extract the best estimates of parameters, usually with over-determined data where we have many more equations than variables.

The last two applications may be combined for a definition of geophysical inversion that produces "models of the earths physical properties", (Lines and Levin 1992), from observations collected at the earth's surface or in a borehole. These processes include:

- Lindseth's (1979) method of estimating acoustic impedance by combining an "integrated" seismic trace with a low frequency velocity model,
- Line's et al (1988) method for estimating horizons and velocities from seismic and potential field data, or a
- Kirchhoff type migration that attempts to produce a reflectivity image of the subsurface from seismic data.

Figure 1a illustrates the forward modelling process in which seismic data is created from reflectivity and a wavelet. Figure 1b illustrates the reverse process of inversion in which geological data is *estimated* from the seismic data.

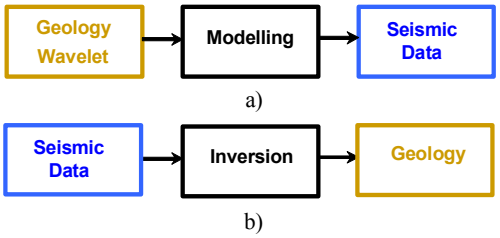

Figure 1. Illustrations of a) the forward modelling process and b) the reverse or inversion process.

The forward modelling process uses established principles of physics to create "exact" seismic data. However, the reverse process is more difficult, because we don't know the wavelet, and some operations are arithmetically inverted with the possibility of division by zero. Approximations may be included in the inversion process to stabilize the results.

In contrast to inversion, seismic migration is a process that uses the wave equation to reposition or focus seismic energy at a location that represents the reflectors.

Kirchhoff migration is based on the integral solution to the wave equation and has kinematic and amplitude parts to the solution. Every migrated sample results from the amplitude weighting and summing of energy along a diffraction shape that is defined by the location of the migrated sample. Modern inversion techniques (Bleistein et al. 2001) also result in the same Kirchhoff type solution, but require "true amplitude" type processing and may apply different amplitude weightings along the diffraction.

Convolutional model and geophysical inversion

We start with the convolutional model for a one dimensional trace to illustrate the inversion process and then proceed to a 2D model with a number of seismic traces with the intent of using the same inversion process to estimate the reflectivity.

The seismic data *s(t)* is formed by convolving the reflectivity in time *r(t)* with a wavelet *w(t)*, i.e., $s(t) = r * w(t)$. (1)

Expressed in the frequency domain, equation (1)becomes a product, i.e., $S(f) = R(f) \bullet W(f)$. (2)

This linear form of the equation enables a simple estimation of the reflectivity at each frequency from $$R(f)=\frac{S(f)}{W(f)}. \quad (3)$$

The reflectivity could be found by summing all the frequency components using the Fourier transform. The problem with this procedure is that *W(f)* may go to zero at some frequency, preventing the division in equation (3). With inversion, as in deconvolution, the procedure becomes an estimation problem that is solved with a variety of methods.

Linearization of convolution using matrices

We linearized the convolution process above by using the frequency domain. Convolution can also linearize with matrix theory. We start with a one dimensional model where the reflectivity, wavelet, and trace are functions of time as defined by the convolution equation

$$s(t)=\int_{-\infty}^{\infty} r(\tau)*w(t-\tau)d\tau, \quad (4)$$

where we integrate over τ to compute *one* sample on the seismic trace *s(t)*, as illustrated in Figure 2. Corresponding time samples in *r* and *w* are first multiplied then summed to get the single nth sample, i.e. the dot product. We then compute all values of *t* (or *n*) on the trace to complete the convolution.

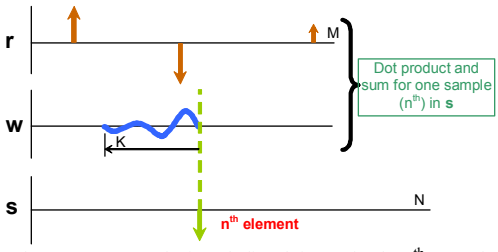

Figure 2. Convolution defined for a single nth sample.

All elements of the seismic vector can be computed by repeating the process for all values of *n*, as illustrated in Figure 3 that shows numerous wavelets with varying delays. In this cartoon figure, (and those that follow), the sample interval is much finer along the rows to define the wavelet than between the rows for illustration purposes, but the intent is to imply that the reversed wavelet increases one sample to the right when progressing to the next row, i.e. at the *nth* row, the right side of the wavelet is at the *nth* sample. The sample-by-sample "dot" product of the reflectivity vector with the wavelet at the *nth* row, (containing the enlarged wavelet in blue), is summed, then stored at the *nth* location in the seismic vector.

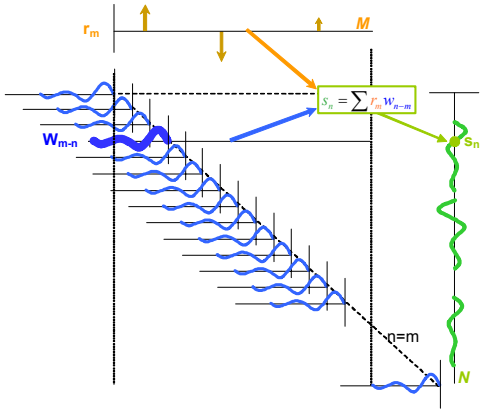

Figure 3 Computing other samples in the

The wavelet data illustrated in Figure 3 is in a convenient form to be defined by a two dimensional matrix **W** that has *N* rows and *M* columns, with the number of columns defined to match the number of elements in the reflectivity vector. Each row in the matrix defines at least a portion of the delayed and time reversed wavelet w_{m-n}, where *n* represents the row number and *m* the column number. All the elements on a given diagonal of **W** will be the same, i.e. **W** is a Toeplitz matrix. To be consistent with matrix algebra, we define the reflectivity as a column vector **r**, and the seismic trace as a column vector **s**. The matrix equation for the convolution process then

becomes a linear process $$\underset{[N\times M]}{\mathbf{W}}\ \underset{[M]}{\mathbf{r}} = \underset{[N]}{\mathbf{s}} \quad (5)$$

where, for convenience, the dimensions are shown in square brackets below the matrix and vectors.

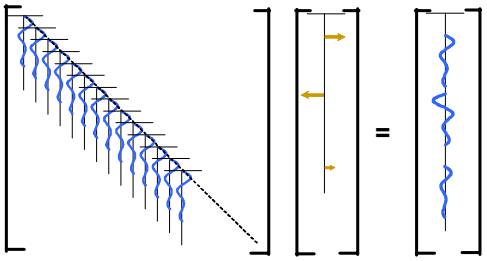

Figure 4 Matrix form of the convolutional model

Equation (5) is visualized in Figure 4 similar to that in Margrave 1998, where the wavelets are shown plotted with vertical traces. This description of the process is in the impulse response form where the wavelet is summed into the model trace with a weighting proportional to the amplitude of the reflector.

We now have two methods of modelling. First we have convolution where each output sample is defined directly by the dot-product (integration or correlation) with a horizontal slice through the wavelet matrix. Second we have the impulse response method where the output trace is composed of summing the impulse responses, but we have to wait until all wavelets are summed before we have any completed output samples.

These two concepts are very significant when modelling seismic data as output points may be formed by summing energy in semi-circles, i.e. the convolution process, or by spreading energy on diffractions, the impulse response method. In migration, the convolution process sums energy in a diffraction, while the impulse response method spreads energy along a semicircle.

Reversing the modelling process

It was easy to do the forward modelling where the seismic trace was computed from a reflectivity and wavelet using equation (5). We now "reverse" this modelling process to estimate the reflectivity from a given seismic trace and known wavelet. Let's start by trying to take the inverse of **W** in equation (5) to get $$\underset{[M]}{\mathbf{r}} = ?\ \underset{[M\times N?]}{\mathbf{W}^{-1}}\ \underset{[N]}{\mathbf{s}}. \quad (6)$$

That probably won't work because we can't take the inverse of a matrix that is not square, and we would have to make $M = N$. That could be solved, but the biggest problem is that **W** may contain zeros, which, when inverted, would become unstable. There are a number of ways to modify **W** to make it invertible, such as adding small numbers to eliminate the zeros (such as pre-whitening), however, we will consider an alternate solution known as the "Least Squares" method.

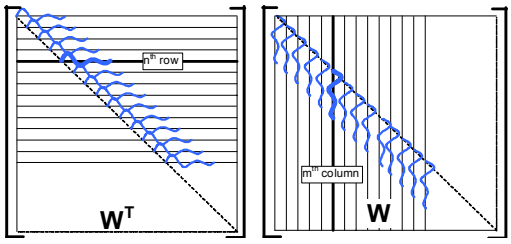

Figure 5 Illustration of W^T and W with corresponding rows and columns displayed for taking the product of the two matrices.

Least squares solution

One solution to the inverse problem is to multiply both sides of equation (5) by the transpose of **W**,

$$\underset{[M\times N][N\times M][M]}{\mathbf{W}^T\ \mathbf{W}}\ \underset{[M]}{\mathbf{r}} = \underset{[M\times N][N]}{\mathbf{W}^T\ \mathbf{s}}, \qquad (7)$$

and then inverting $\mathbf{W^TW}$ giving the well known solution (for example Lines and Treitel, 1984, Claerbout 1992).

$$\underset{[M]}{\mathbf{r}} = \left(\underset{[M\times N][N\times M]}{\mathbf{W}^T\ \mathbf{W}}\right)^{-1}\ \underset{[M\times N][N]}{\mathbf{W}^T\ \mathbf{s}}. \qquad (8)$$

The product $\mathbf{A} = \mathbf{W^TW}$ produces a square matrix which can be inverted only when there are no zeros in the spectrum of the auto-correlation wavelet.

The square matrix **A** is shown in Figure 6a with vertical traces that illustrate that all the new wavelets are the delayed auto correlation of the original wavelet. Plotting the data with horizontal traces should produce the same image (with adequate column sampling).

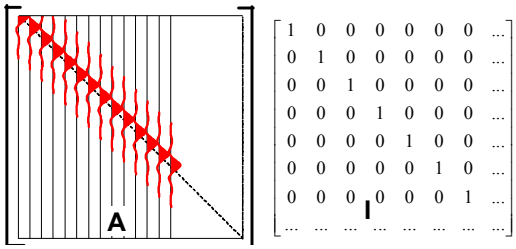

a) b)

Figure 6 The result of $A = W^TW$, the product of a matrix and its transpose in a) and in b) the identity matric I.

All elements on any diagonal in **A** are equal (i.e. Toeplitz) with the largest value on the diagonal. This is very significant as **A** is similar to the identity matrix **I** in which the data is zero, except for unit values on the diagonal, as illustrated in Figure 6b.

A feature of the identity matrix is that the inverse is also an identity matrix, i.e. $\mathbf{I^{-1}} = \mathbf{I}$. If we assume that the auto-correlation matrix **A** is an approximation to the identity matrix **I** (except for a scale factor), we can now assume

$$\underset{[M\times N][N\times M]}{\mathbf{W}^T\ \mathbf{W}} = \underset{[M\times M]}{\mathbf{A}} \approx \underset{[M\times M]}{\mathbf{I}}, \qquad (9)$$

and also that

$$\left(\underset{[M\times N][N\times M]}{\mathbf{W}^T\ \mathbf{W}}\right)^{-1} \approx \underset{[M\times M]}{\mathbf{I}}. \qquad (10)$$

This simplification allows equation (8) to be reduced to the very simple form

$$\underset{[M]}{\mathbf{r}} \approx \underset{[M\times N][N]}{\mathbf{W}^T\ \mathbf{s}}, \qquad (11)$$

estimating the reflectivity $\hat{\mathbf{r}}$ by

$$\underset{[M]}{\hat{\mathbf{r}}} = \underset{[M\times N][N]}{\mathbf{W}^T\ \mathbf{s}}. \qquad (12)$$

The reflectivity is estimated from the product of the seismic vector **s** with the transpose of the wavelet matrix $\mathbf{W^T}$. Our simplifications have assumed that the inverse to a matrix $\mathbf{W^{-1}}$ can be approximated by a very simple transpose $\mathbf{W^T}$, i.e.,

$$\underset{[M\times N]}{\mathbf{W}^T} \approx \underset{[M\times N?]}{\mathbf{W}^{-1}}. \qquad (13)$$

The simplifications leading to equation (13), produce a band-limited form of the reflectivity.

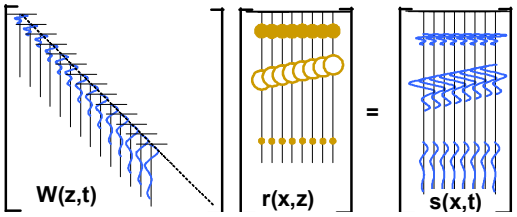

Figure 7 Matrix form of the convolutional model with time varying wavelets.

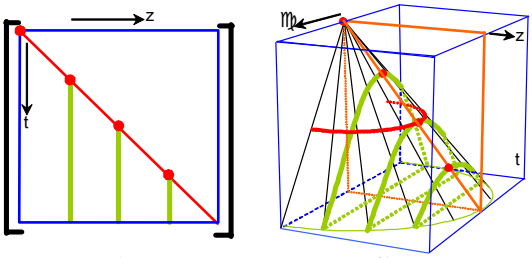

a) b)

Figure 8 The diffraction matrix D in the (z, t) view in a) and a perspective view b) showing the dimension of χ.

KIRCHHOFF MIGRATION AS A TRANSPOSE PROCESS

In seismic modelling we place a diffraction at every scatterpoint. When Kirchhoff migrating, we define a kinematic diffraction shape at a scatterpoint, then weight and sum the input energy at locations defined by this diffraction shape. The summed energy is then insert at the scatterpoint location. This is a two-dimensional cross correlation, and will produce a peak of energy when a migration diffraction matches a diffraction in the input data. This Kirchhoff migration corresponds to a *transpose* process that approximates true inversion.

Visualizing modelling data with diffractions

We start by modelling a gather of reflectivity traces with a wavelet matrix **W** in which the wavelets are *time varying* to get a gather of traces **s** as illustrated in Figure 7. Note that the reflectivity **r** is now defined correctly with a depth component, along with non-stationary wavelets that vary with depth.

We now replace the time varying wavelet with a time varying diffraction that requires an added dimension of χ to account for the number of traces in the diffraction, giving a 3D matrix $\mathbf{D(\chi, z, t)}$. A side view is shown in Figure 8a that shows the diffraction as a time varying "wavelet", similar to that in Figure 7. The full 3D diffraction model is illustrated in Figure 8b,

which shows the kinematic shape of three diffractions. The **D** matrix is mainly composed of null space, with scaled values on a surface, which, when the velocities are constant, is a cone with a vertical axis.

Seismic modelling is illustrated in Figure 9 where one sample in **S** at $s(x_p, t_q)$ is formed when the 2D matrix **R** is dot multiplied by one plane of the 3D diffraction matrix **D** at constant time t. The matrix **R** is aligned such that the location of the migrated trace (in red) coincides with the location of $\chi = 0$, as illustrated in Figure 9. This figure also shows the $\mathbf{R}^T$ matrix above the diffraction matrix **D**. As different migration traces are selected, the matrix $\mathbf{R}^T$ above **D** is shifted in the corresponding χ direction.

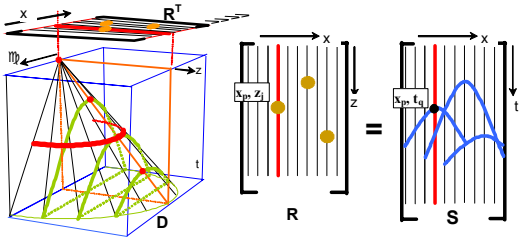

Figure 9 A zero-offset section S from a reflectivity matrix R and a diffraction matrix D.

The time of a modelled sample t_q is selected by the horizontal plane within **D**, and the trace location x_p by the relative alignment of that trace above $\chi = 0$ as given by

$$s(x_p,t_q) = \sum_{\chi_i=-I}^{I} \sum_{z_j=1}^{J} d(\chi_i,z_j,t_q) r\left(x_p - \chi_i, z_j\right), \quad (14)$$

or

$$\underset{[x,z,t][x,z]}{\mathbf{D}} \; \underset{[x,z]}{\hat{\mathbf{r}}} = \underset{[x,t]}{\mathbf{s}} . \quad (15)$$

A constant time (slice) in **D** intersects the diffraction cone at a semi-circle, identified by one red curve in the perspective view of Figure 9. This corresponds to modelling a seismic section by summing over a semi-circle.

Matrix theory shows what happens to equation (15) when we take the transpose of **D** by interchanging z and t (illustrated in Figure 10) to estimate a migrated section from a zero-offset section,

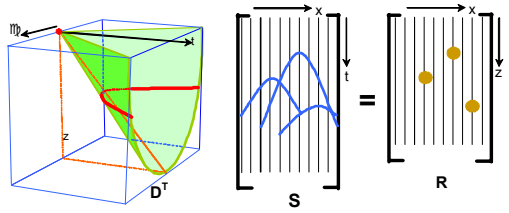

Figure 10 A reflectivity matrix R estimated from a transpose diffraction matrix D^T and seismic data S.

i.e.,

$$\underset{[x,z]}{\hat{\mathbf{r}}} = \underset{[x,z,t][x,t]}{\mathbf{D}^{\mathbf{T}}} \; \underset{[x,t]}{\mathbf{s}} . \quad (16)$$

The section **s** is dot multiplied with constant depth planes (slices) and the energy is summed where the horizontal plane intersects the cone, illustrated at one depth level by a red hyperbola. The equation for migrating one sample $r(x_p, z_q)$ is

$$\hat{r}(x_p,z_q) = \sum_{\chi_i=-I}^{I} \sum_{t_j=1}^{J} d(\chi_i,z_q,t_j) s\left(x_p - \chi_i, t_j\right). \quad (17)$$

COMMENTS AND CONCLUSIONS

The diffraction matrix illustrated in Figure 8 shows the constant velocity diffractions on a cone. These diffractions can be modified to be time varying by using RMS velocities with shapes illustrated in Figure 11a.

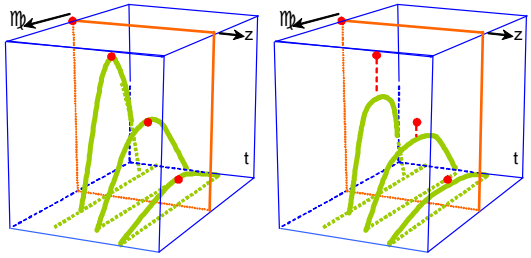

Figure 11 a) Time varying diffractions and b) and offset diffractions.

The diffraction shapes can also be modified to contain constant-offset diffractions as illustrated in Figure 11b. Modelling will then produce a constant-offset section. The inversion of an offset section would therefore use the transpose of the offset diffractions.

The kinematics of diffraction stack migrations are straight forward. Matched filtering suggests that the amplitude weightings used, when summing the diffractions, should match the diffraction amplitudes on the seismic data. These weightings are similar to those obtained from the Kirchhoff integral solution to the wave equation (Schneider1978).

Inversion techniques provide an alternate solution when imaging the subsurface, and in some cases produce algorithms that are very similar to Kirchhoff migrations. Simplifications to the least squares inversion process showed that Kirchhoff migration is a transpose process that approximates inversion.

ACKNOWLEDGMENTS

I wish to thank NSERC and the Consortium for Research in Elastic Wave Exploration Seismology (CREWES) for their support of this work.

REFERENCES

Bleistein, N., Cohen, J. K., and Stockwell, Jr., J. W., 2001, Mathematics of Multidimensional Seismic Imaging, Migration, and Inversion, Springer

Claerbout, J. F., 1992, "Earth Soundings Analysis: Processing versus inversion", Blackwell Scientific Publications

Lindseth, R. O., 1979, Synthetic sonic logs-a process for stratigraphic interpretation, Geophysics, 44, 3-26

Lines, L. R., and Levin, F. K., 1992 Inversion of Geophysical Data, Geophysical reprint series, No. 9, SEG

Lines, L. R., and Treitel, S., 1984, Tutorial: a review of least-squares inversion and its application to geophysical problems, Geophysical Prospecting, 32, 159-186

Margrave, G F., 1998, Theory of non-stationary linear filtering in the Fourier domain with applications to time-variant filtering, Geophysics, 63, 255-259

Schneider, W. A., 1978, Integral formulation for migration in two and three dimensions, Geophysics, 43, 49-76